International Journal of Electrical and Computer Engineering (IJECE)
Vol. 15, No. 5, October 2025, pp. 4593~4604
ISSN: 2088-8708, DOI: 10.11591/ijece.v15i5.pp4593-4604

Decomposition and multi-scale analysis of surface electromyographic signal for finger movements

Afroza Sultana[1], Md. Tawhid Islam Opu[1], Md. Shafiul Alam[2], Farruk Ahmed[3]
[1]Department of Electrical and Electronic Engineering, Independent University, Dhaka, Bangladesh
[2]Department of Electrical and Electronic Engineering, University of Dhaka, Dhaka, Bangladesh
[3]Department of Computer Science and Engineering, Independent University Bangladesh, Dhaka, Bangladesh

Article Info

Article history:

Received Dec 21, 2024
Revised Jun 23, 2025
Accepted Jun 30, 2025

Keywords:

Decomposition
Finger movements
sEMG signal
Wavelet transform
reconstruction

ABSTRACT

Decomposition of the surface electromyography (sEMG) signal is vital for separating the composite, complex, noisy signals recorded from muscles into their integral motor unit action potentials (MUAPs). By precisely identifying each motor unit's activity, this method offers greater insights into the functioning of the neuromuscular system, which helps isolate each motor unit's contribution, making it essential for understanding muscle coordination and diagnosing neuromuscular disorders. In this study, we employ the maximal overlapping discrete wavelet transform (MODWT), which is well-suited for analyzing signals in the time-frequency domain. The study decomposed the sEMG signal into six levels to identify the neural activity of finger movements and analyzed the motor unit action potential (MUAP). In the frequency range of 30.2 and 64.6 Hz, the signal exhibits the highest MUAP which is independent of movement. Using inverse MODWT, it was rebuilt from the decomposed levels. With 95.8% accuracy, the similarity between the reassembled signal and the original signal was determined using correlation analysis to assess the efficacy of the method.

Corresponding Author:

Afroza Sultana
Department of Electrical and Electronic Engineering, School of Engineering Technology and Sciences, Independent University Bangladesh (IUB)
Plot-16, Block B, Aftabuddin Ahmed Road, Bashundhara R/A, Dhaka-1229, Bangladesh
Email: afroza@iub.edu.bd

1. INTRODUCTION

Surface electromyography (sEMG) is a flexible and non-invasive method for estimating muscle force, which has been utilized in neuromuscular physiology, movement disorder investigation, control of assistive devices such as prosthetic hands, and for diagnosing neuromuscular diseases. Information about muscle movements and neural activity is obtained by measuring the electric currents produced in muscles during contraction. The raw EMG signal is a mixture of overlapping motor unit action potentials (MUAPs) from multiple muscle fibers. Decomposing this complex signal helps isolate individual MUAPs, allowing researchers and medical professionals to analyze the contribution of specific motor units for a more accurate assessment of muscle health and function. In physiological research, motor unit features and muscle motor control mechanisms are studied using both the MUAP waveform characteristics and the statistics of the inter-pulse intervals [1]. The unique characteristics of a degraded MUAP can yield important information about the state of the nervous system—information that is necessary for clinically diagnosing myopathies and neuropathies [2], stroke patients [3], research into the neuromuscular control loop [3], and the prediction of human movements in prosthetics and exoskeletons [4], [5]. Decomposition of sEMG data into motor unit discharge patterns provides information on the recruitment and discharge behavior of motor neurons for investigating the neural control of movement.

Decomposition of EMG signals requires a technique that can handle four levels of complexity: changing action potentials due to sensor movement, similar shapes at different times, superimposed action potentials, and a wide dynamic range of amplitudes, making the decomposition process more challenging [6]. Various decomposition approaches, such as blind source separation (BSS), convolution kernel compensation (CKC), independent component analysis (ICA), empirical mode decomposition (EMD), and the Fourier decomposition method (FDM) that have been used for several decades to decode motor neuron activities in the sEMG-based system.

Negro *et al.* [7] and Mohebian *et al.* [8] applied the convolutive BSS method in decomposition algorithms to segregate individual motor unit action potentials. The BSS method of sEMG enhances motor unit study with non-invasive recordings, but challenges persist, including varying success rates across conditions, muscles, and individuals [9]. Besides, it brings substantial challenges due to its unique characteristics, including low signal-to-noise ratio, high similarity, and severe superposition of MUAP waveforms [10]. The EMD base decomposition was used by Wei *et al.* [11] for the recognition of lower limb movements, but EMD has limitations due to the mix-mode effect brought on by intermittent signal components [12]. The mix-mode effect was addressed by an enhanced version called ensemble EMD (EEMD), which also brought the difficulty of including residual supplemental noises during signal reconstruction [13]. Fatimah *et al.* [14] applied the Fourier decomposition method to decompose the surface EMG signal for the recognition of hand gestures. Fourier analysis's assumption of signal stationarity results in inaccurate frequency representation over time and lacks time resolution, making it challenging to track transient features like muscle activation patterns. Chen *et al.* [15] applied the CKC method for individual segments to decode the motor unit discharges from each motor neuron. According to the studies [16] [17] when more motor activities are involved, the traditional CKC approach is unable to find enough MUs for myoelectric control. The wavelet transform decomposition method was used by Liu *et al.* [18] and Duan *et al.* [19] and Phinyomark [20] to recognize different hand motions for prosthetic hands. Wavelet-based methods have advanced, but have drawbacks like dependency on wavelet function selection, inability to combine smoothness with numerical characteristics, and difficulty handling non-stationary EMG signals, limiting precise denoising and reconstruction [21]–[23].

This study uses a multiresolution decomposition method based on the maximal overlapping discrete wavelet transform (MODWT) to offer adequate denoising and reconstruction of multi-class EMG signals. Because of its improved noise reduction capabilities using the wavelet coefficient, the MODWT is a suitable method for more accurate multiresolution analysis of complex, noisy data [24]. The main contribution of this research is:

a. The work proposes a novel technique based on multiresolution decomposition using MODWT for the appropriate denoising decomposition and reconstruction of multi-class EMG signals.
b. The method potentially identified the specific frequency band where the motor neurons activate during different movements of single and multiple fingers.
c. Identified the dominant channels from eight-channel sEMG data by effectively measuring the average relative energy.

2. MATERIALS AND METHODS

2.1. Work flowchart

The research work was completed in several phases. The different phases of the work are presented by a flow diagram in Figure 1.

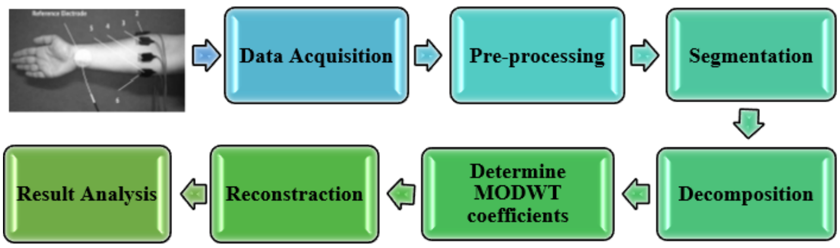

Figure 1. Flow diagram of the work

2.2. Data acquisition

This study made use of the dataset obtained from Khushaba and Kodagoda [25] where fifteen classes of movement data were obtained from eight volunteers (six males and two females, aged between 20 to 35) using 8 channels. Fifteen classes of movements were collected during the flexion of each of the individual fingers, *i.e.*, thumb (TT), index (II), middle (MM), ring (RR), little (LL), and the combined fingers-thumb-index (TI), thumb-middle (TM), thumb-ring (TR), thumb-little (TL), index-middle (IM), middle-ring (MR), ring-little (RL), index-middle-ring (IMR), middle-ring-little (MRL), and hand close class (HC).

2.3. Preprocessing and segmentation

The sEMG signals are often tainted by background noises caused by electronic equipment, subject movements, and physiological factors. Proper detection and processing using efficient and cutting-edge techniques can be a basic prerequisite for its use in various domains. The EMG power spectrum can be shaped using a variety of band-pass, notch, high-pass, and low-pass filters. Typically, surface EMG signals are band-pass filtered between 20 Hz and 500 Hz to remove noise at frequencies below 20 Hz and above 500 Hz [26]–[28]. In this study, the collected data was sampled at 4000 Hz, amplified to a total gain of 1000 dB, and to eliminate the 50 Hz line interference, the signal was band-pass filtered with a 20 Hz to 450 Hz filter. To reduce processing time, the preprocessed signal must be extracted based on a threshold to determine the part of the signal that corresponds to each movement [29]. Therefore, the collected signal is sectioned into four non-overlapping segments of equal length, and the segment with the highest PSD is considered for decomposition.

2.4. Decomposition using maximal overlapping discrete wavelet transform

The time-frequency analysis method evaluates time-varying non-stationary signals using the wavelet transform, which uses orthogonal bases with different resolutions. It distributes signal decomposition in narrow frequency bands, filters without altering patterns, and handles time domain data without compromising frequency domain precision [30]. The MODWT is a DWT variation that uses a high-pass and low-pass filter to decompose a time signal into detailed and approximation signals, allowing for multiresolution analysis of smooth and detailed coefficients [31]. MODWT performs multi-resolution analysis of a signal, which is a scale-based additive decomposition like DWT. Within precise and approximative components, the MODWT module does not generate phase changes [32]. The MODWT filters the input signal according to the number of levels at which it eliminates the noise coefficients from the signal. MODWT offers flexibility in signal starting points, can handle any sample size, and is more efficient than DWT as its smooth and detailed coefficients are associated with zero-phase filters [33]. For noisy data analysis, MODWT frequently uses the Daubechies wavelet function, and it provides a balance in the time-frequency localization [34]. The Daubechies wavelet function in MODWT yields the least error and allows for more coherent structure extraction compared to the Haar, Coiflet, Symmlet, and Biorthogonal functions [35], [36], and is therefore used in this analysis. MODWT splits the frequency spectrum of the input signal into scaling and wavelet coefficients, as shown in Figure 2. Any segmented signal N that is an integer multiple of 2j, for $j = 1, 2, 3, \dots J$ can be implemented using the MODWT, where J is the level and j is the scale of the decomposition.

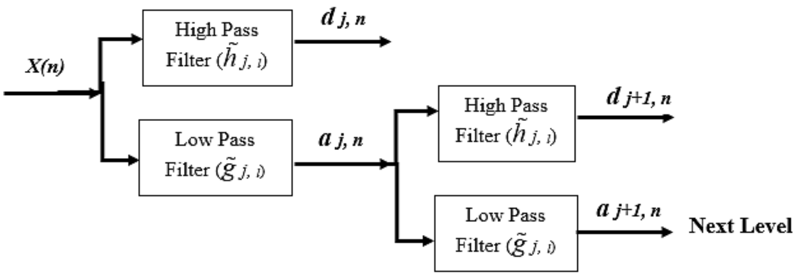

Figure 2. Wavelet decomposition

The MODWT scaling filters $\tilde{h}_l$ and wavelet filters $\tilde{g}_l$ are represented as [34], [37].

$$\tilde{h}_l = \frac{hl}{\sqrt{2}} \tag{1}$$

$$\tilde{g}_l = \frac{gl}{\sqrt{2}} \tag{2}$$

The quadrature mirror filters used in MODWT are expressed as (3) and (4),

$$\tilde{h}_l = (-l)^{l+1} h_{L-1-l} \quad (3)$$

$$\tilde{g}_l = (-l)^{l+1} g_{L-1-l} \quad (4)$$

where l=0, 1, 2, ..., $L-1$, and L is the length of the wavelet filter.

The nth element of the first-stage wavelet coefficients ($\tilde{W}_{l,n}$) and scaling coefficients ($\tilde{V}_{l,n}$) of MODWT with the input time series signal $X(n)$ is presented as (5), (6),

$$\tilde{W}_{l,n} = \sum_{l=0}^{L1-1} \tilde{h}_l \; X_{n-l \bmod N} \quad (5)$$

$$\tilde{V}_{l,n} = \sum_{l=0}^{L1-1} \tilde{g}_l \; X_{n-l \bmod N} \quad (6)$$

where n=1, 2, 3, ..., N, and N is the length of the signal in a sample to be analyzed. The equations (7) and (8) can be used to calculate the first-level approximations and details.

$$\tilde{A}_{l,n} = \sum_{l=0}^{L1-1} \tilde{g}_l \, X_{n-l \bmod N} \quad (7)$$

$$\tilde{D}_{l,n} = \sum_{l=0}^{L1-1} \tilde{g}_l \; \tilde{W}_{l,n+l \bmod N} \quad (8)$$

For a time, series X of random sample size N, the j^{th} level MODWT wavelet coefficients ($\tilde{W}_{jn}$) and scaling coefficients ($\tilde{V}_{jn}$) are defined in (9) and (10):

$$\tilde{V}_{jn} = \sum_{l=0}^{L1-1} \tilde{g}_{j,l} \; X_{n-l \bmod N} \quad (9)$$

$$\tilde{W}_{jn} = \sum_{l=0}^{L1-1} \tilde{h}_{jl} \; X_{n-l \bmod N} \quad (10)$$

Similarly, equation (11) and (12) give the approximations Aj and the details D_j of the n^{th} element of the j^{th} stage MODWT.

$$\tilde{A}_{j,n} = \sum_{l=0}^{L1-1} \tilde{g}_l \, X_{n-l \bmod N} \quad (11)$$

$$\tilde{D}_j, n = \sum_{l=0}^{L1-1} \tilde{h}_l \; \tilde{W}_{l,n+l \bmod N} \quad (12)$$

where $\tilde{g}_l$ is the MODWT wavelet filter periodized to length N and $\tilde{h}_l$ is the MODWT scaling filter periodized to length N. Thus, the original time series signal can be expressed using the following estimates and details:

$$X(n) = \sum_{l=0}^{j} \tilde{D}_J + \tilde{A}_J \quad (13)$$

The fundamental block diagram of MODWT is shown in Figure 3, and the complete procedure is explained in Algorithm 1.

2.5. Reconstruction using inverse maximal overlapping discrete wavelet transform (MODWT)

Restoring a continuous-time signal from discrete samples is known as signal reconstruction. To reconstruct the signal, the approximation and detail coefficients at each level must be combined again. The inverse transform reconstructs the detail and approximation coefficients for every level j and is expressed as:

$$X(t) = \sum_{j=1}^{J} (InverseMODWT(\tilde{D}_j(t)) + InverseMODWT(\tilde{A}_j(t))) \quad (14)$$

The inverse MODWT uses the scaling filters $\tilde{h}_l$ and wavelet filters $\tilde{g}_l$ to reverse the decomposition using:

$$X(n) = \sum_k \tilde{A}j[k] \, \tilde{h}_{J-k}(t) + \sum_{j=1}^{J} \sum_k \tilde{D}j[k] \, \tilde{g}_{j-k}(t) \quad (15)$$

By recombining all detail coefficients and approximation levels, the inverse MODWT reconstructs the original signal while preserving its length and resolution [34].

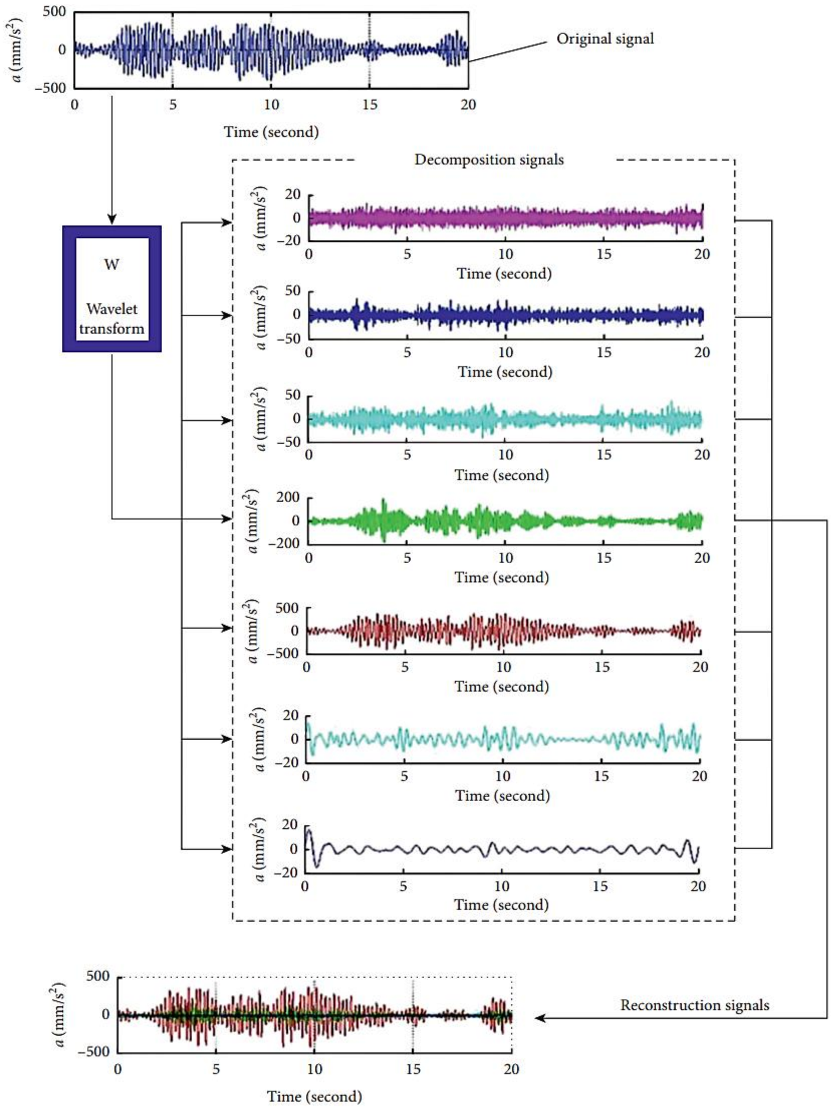

Figure 3. Decomposed and reconstructed signal using MODWT [38]

Algorithm 1. Algorithm of sEMG signal decomposition and reconstruction

```
Initialization
 • Input the sEMG signal X(t) of length N.
 • Specify the level of decomposition J.
 • Select the wavelet filter
Decomposition using MODWT
 1. For l=1, 2..., L
 2. Apply the MODWT scaling filter h̃_l to obtain approximation coefficients Ã_l
 3. Apply the MODWT wavelet filter g̃_l to extract detail coefficients D̃_l
 4. Repeat steps 1 to 3 for all levels l until the maximum level L is reached
 5. Store the approximation coefficients Ã_l from the highest level and the detail
    coefficients D̃_l from each level l
Reconstruction using Inverse MODWT
 1. Initialize the reconstructed signal X_r(t) as a zero vector of length N.
 2. Reconstruct the signal using the approximation and detail coefficients from all levels:

        X_r(t)=Ã_l(t)

 3. For each level l=1, 2..., L, reconstruct the contribution from the detail coefficients:

        X_r(t)= X_r(t) + D̃_l (t)

 4. End
```

3. RESULTS AND ANALYSIS

The sEMG signal was decomposed with multiresolution analysis methods using a 4^{th}-order Daubechies filter (db4) up to level 6. Upon increasing the levels from 4 to 7, we found that the optimal results were obtained at level 6. Inverse MODWT was used to reconstruct the original signal. The frequency range that matched the detail and approximation coefficients at each wavelet level of decomposition is displayed in Table 1, and the result of decomposition is presented in Figure 4, where Figure 4(a) represents the original signal and Figure 4(b) shows the decomposed signals.

To identify the possible frequency range of MU firings and find the relative energy at each level, we decomposed the dataset for each of the fifteen classes of movement. Table 2 presents the results of decomposition for each class of movement signal from different channels, and Table 3 displays the results of the average MUAP for all 15 classes, considering all subjects.

Table 1. Frequency band corresponding to each wavelet level

Decomposition level	Frequency range (Hz)	Bandwidth (Hz)	Overlapping frequency (Hz)
Level-1	1000- 2000	1000	40
Level-2	483 -1040	557	34
Level-3	241 - 517	276	17
Level-4	121 - 258	137	8
Level-5	60.3-129	68.7	4.3
Level-6	30.2-64.6	34.4	
Approx.	0-31.1		

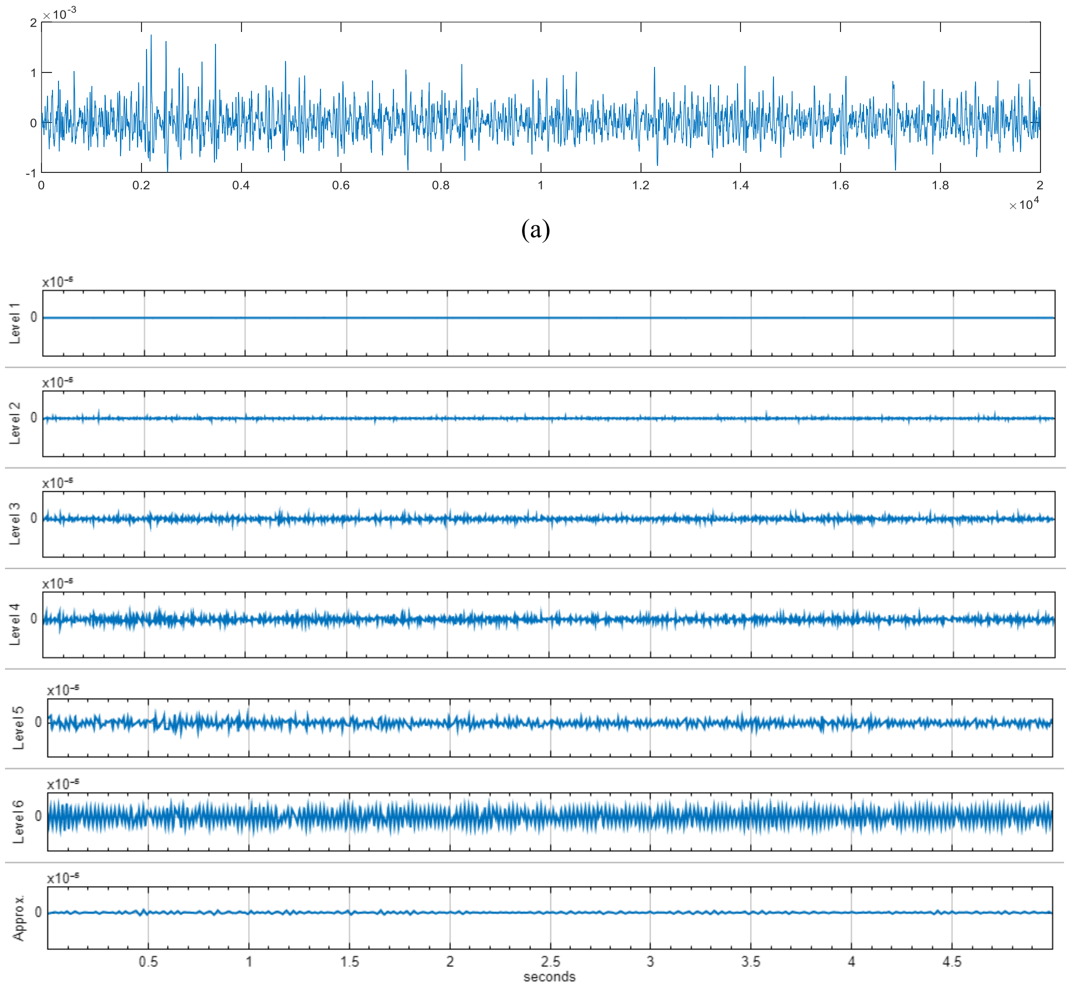

(a)

(b)

Figure 4. Decomposition using MODWT (a) original sEMG signal and (b) signal after decomposition into 6 levels

Table 2. The percentage of the relative energy of the decomposed signal for different movements (Sub-2)

Freq levels	HC	II	IM	IMR	LL	MM	MR	MRL	RL	RR	TI	TL	TM	TR	TT
Level-1	0.01	0.01	0.03	0.01	0.01	0.02	0.02	0.01	0.01	0.01	0.01	0.01	0.02	0.01	0.01
Level-2	0.43	0.58	0.96	0.50	0.50	0.75	0.60	0.49	0.44	0.45	0.52	0.38	0.59	0.45	0.62
Level-3	4.84	5.40	6.42	4.63	5.05	6.76	5.25	4.21	3.61	4.38	5.18	3.95	5.32	4.41	5.80
Level-4	18.27	14.58	14.10	13.12	15.09	14.77	12.02	11.69	10.54	13.78	16.11	14.51	17.24	15.73	15.53
Level-5	34.81	28.93	27.99	30.87	32.41	28.25	27.58	28.73	30.28	31.75	34.71	31.60	33.19	34.72	29.27
Level-6	37.10	42.91	42.57	46.45	40.36	42.36	48.93	50.99	50.20	42.65	38.52	44.35	38.47	39.61	41.45
Approx.	4.55	7.59	7.94	4.43	6.58	7.10	5.60	3.82	4.92	6.98	4.96	5.20	5.19	5.02	7.31

Table 3. Average of the relative energy for different motor neuron activities (Ch-2)

Freq levels	HC	II	IM	IMR	LL	MM	MR	MRL	RL	RR	TI	TL	TM	TR	TT
Level-1	0.02	0.02	0.01	0.02	0.01	0.01	0.01	0.01	0.01	0.01	0.01	0.01	0.02	0.01	0.01
Level-2	0.89	0.72	0.88	1.00	0.48	0.55	0.73	0.30	0.20	0.44	0.66	0.54	0.96	0.52	0.78
Level-3	7.42	9.94	10.83	9.27	6.92	8.06	7.69	2.20	2.91	6.39	7.77	7.35	9.94	6.85	8.95
Level-4	11.61	28.35	26.66	14.86	25.87	27.78	13.71	3.62	16.20	25.95	24.48	27.84	22.95	24.72	26.68
Level-5	21.75	35.63	29.14	21.02	34.79	38.12	21.08	19.67	34.46	37.31	36.88	38.53	30.20	36.61	35.52
Level-6	54.53	21.8	29.94	52.17	27.58	21.45	54.87	73.00	42.14	25.13	25.87	22.44	32.80	27.32	24.15
Approx.	3.87	3.55	2.52	1.66	4.35	4.02	1.9	1.20	4.09	4.77	4.33	3.30	3.13	3.96	3.90

According to the decomposition result, level 6, or the frequency range of 30.2 to 64.6 Hz, showed the maximum concentration of action potentials as shown in Figure 5. Furthermore, we found that neither the subject, as illustrated in Figure 6, nor the specific movement of any subject, as illustrated in Figure 7, affects the average relative energy of any level

For each class of movement, the signal was reconstructed by combining all the decomposed levels using inverse MODWT; the original signal is shown in Figure 8, and the reconstructed signal of the corresponding movement is shown in Figure 9. The signal was also reconstructed from the level-5 and level-6 coefficients, as shown in Figure 10, because the highest energy was found at these levels, and we observed that the resulting signal appears close to the signal reconstructed from the coefficients of all levels.

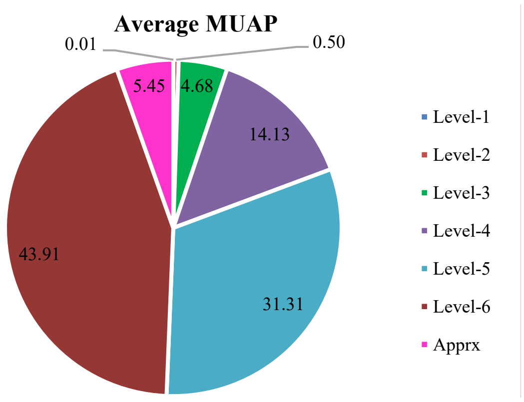

Figure 5. Average MUAP at different frequencies for levels

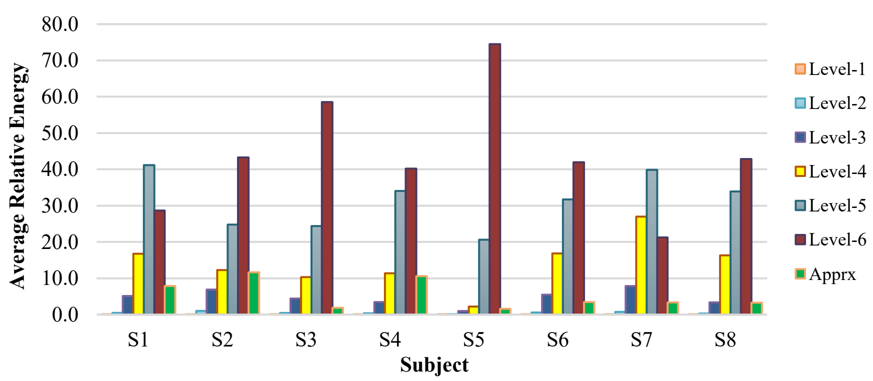

Figure 6. Average MUAP of different frequency levels of different subjects

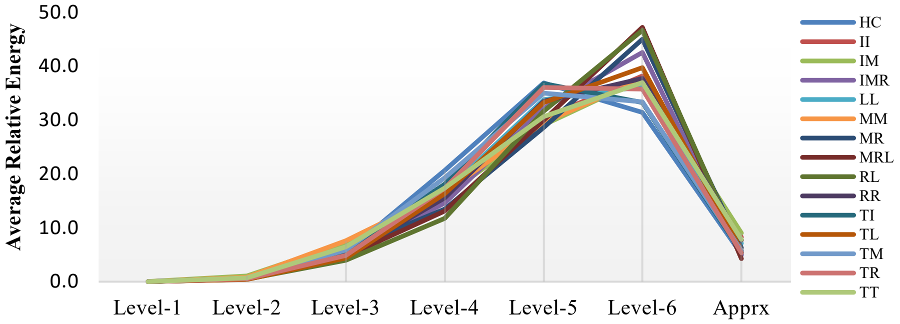

Figure 7. Average MUAP of different frequency levels for different movements

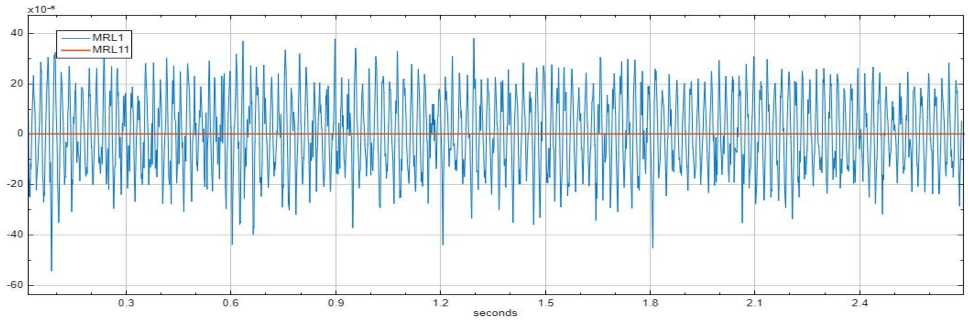

Figure 8. The original surface EMG signal

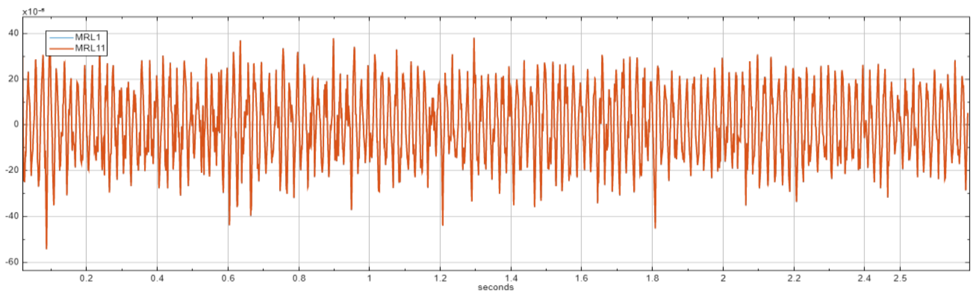

Figure 9. The reconstructed signal with inverse MODWT

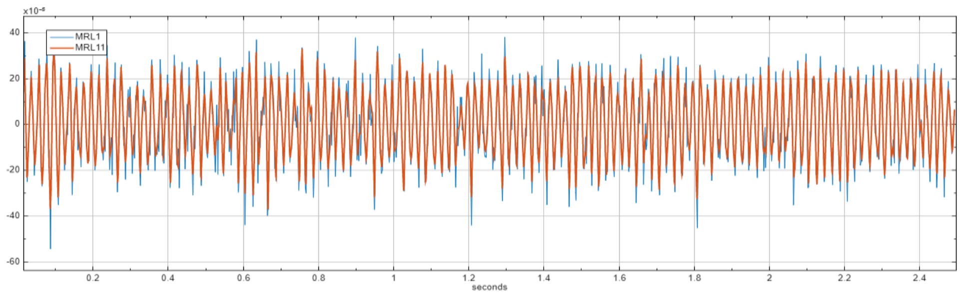

Figure 10. The signal reconstructed from the coefficients of level 5 and level 6

After decomposition and reconstruction of the sEMG signals, we perform a correlation analysis between the original and reconstructed signals to evaluate the accuracy. Correlation analysis is one of the popular techniques for determining the similarities or differences between two sets of multidimensional data. If the shapes of two curves are identical, the cross-correlation coefficient R=1; if not, it will be any value between 0 and 1. Tables 4 and 5 display the value of the correlation coefficients for each of the fifteen classes of data from subjects 4 and 5, and Table 6 shows the average value of the correlation for all subjects.

The average accuracy of decomposition and reconstruction was found to be 95.8%. Figure 11 shows the decomposition accuracy over the fifteen classes of movement. Figure 12 shows the decomposition accuracy of all fifteen classes of movement for all the subjects, respectively.

We investigated the decomposition and reconstruction accuracy results for various movements and channels. About different subjects as shown in Figure 14 and diverse movements as shown in Figure 15, the investigation discovered that channel 2 had the highest average accuracy of 95.8%. The outcome confirms the earlier finding from [39] where Ch-2 and 4 were found to be dominating for the 15 classes of movements during the classification of the movements. This leads to a reduction in overhead and dimensionality, which are crucial to wearable and real-time prosthetic applications.

Table 4. Correlation between the original and reconstructed signals (S-4)

CH	HC	II	IM	IMR	LL	MM	MR	MRL	RL	RR	TI	TL	TM	TR	TT
Ch-1	0.805	0.859	0.839	0.868	0.824	0.867	0.864	0.849	0.867	0.875	0.756	0.751	0.801	0.838	0.857
Ch-2	0.950	0.952	0.950	0.962	0.960	0.952	0.947	0.932	0.947	0.960	0.936	0.978	0.988	0.980	0.967
Ch-3	0.815	0.867	0.849	0.908	0.881	0.867	0.838	0.901	0.900	0.884	0.838	0.874	0.872	0.806	0.863
Ch-4	0.860	0.801	0.817	0.798	0.827	0.819	0.828	0.900	0.848	0.906	0.769	0.791	0.956	0.830	0.824
Ch-5	0.918	0.827	0.809	0.830	0.829	0.816	0.856	0.806	0.815	0.833	0.856	0.817	0.955	0.902	0.807
Ch-6	0.883	0.731	0.666	0.735	0.768	0.731	0.690	0.719	0.734	0.773	0.841	0.652	0.942	0.892	0.769
Ch-7	0.742	0.892	0.845	0.872	0.897	0.873	0.817	0.861	0.721	0.902	0.754	0.875	0.834	0.911	0.881
Ch-8	0.780	0.817	0.804	0.849	0.832	0.815	0.640	0.490	0.478	0.921	0.571	0.854	0.724	0.793	0.820

Table 5. Correlation between the original and reconstructed signals (S-5)

	HC	II	IM	IMR	LL	MM	MR	MRL	RL	RR	TI	TL	TM	TR	TT
Ch-1	0.979	0.964	0.980	0.974	0.812	0.948	0.976	0.979	0.867	0.966	0.837	0.892	0.936	0.871	0.764
Ch-2	0.991	0.991	0.989	0.985	0.981	0.988	0.988	0.991	0.988	0.992	0.987	0.990	0.983	0.981	0.984
Ch-3	0.970	0.973	0.953	0.959	0.956	0.961	0.964	0.951	0.952	0.946	0.961	0.968	0.950	0.954	0.970
Ch-4	0.953	0.958	0.918	0.927	0.939	0.949	0.932	0.928	0.906	0.954	0.950	0.931	0.940	0.918	0.962
Ch-5	0.677	0.781	0.754	0.777	0.854	0.803	0.793	0.787	0.697	0.743	0.895	0.935	0.828	0.781	0.798
Ch-6	0.801	0.730	0.737	0.843	0.713	0.761	0.932	0.757	0.695	0.718	0.930	0.928	0.917	0.755	0.719
Ch-7	0.716	0.880	0.853	0.788	0.882	0.921	0.863	0.914	0.857	0.883	0.917	0.970	0.795	0.855	0.836
Ch-8	0.917	0.907	0.880	0.883	0.903	0.907	0.851	0.920	0.912	0.932	0.888	0.953	0.799	0.910	0.833

Table 6. Average correlation between the original and reconstructed signals

	HC	II	IM	IMR	LL	MM	MR	MRL	RL	RR	TI	TL	TM	TR	TT
S-1	0.932	0.929	0.914	0.899	0.898	0.943	0.980	0.898	0.941	0.939	0.948	0.944	0.899	0.940	0.958
S-2	0.899	0.959	0.893	0.940	0.912	0.949	0.987	0.943	0.945	0.914	0.900	0.957	0.977	0.937	0.976
S-3	0.969	0.987	0.898	0.931	0.939	0.957	0.946	0.911	0.930	0.953	0.927	0.957	0.921	0.936	0.988
S-4	0.950	0.952	0.950	0.962	0.960	0.952	0.947	0.932	0.947	0.960	0.936	0.978	0.988	0.980	0.967
S-5	0.991	0.991	0.989	0.985	0.981	0.988	0.988	0.991	0.988	0.992	0.987	0.990	0.983	0.981	0.984
S-6	0.955	0.845	0.820	0.961	0.973	0.947	0.969	0.967	0.950	0.864	0.867	0.977	0.874	0.868	0.839
S-7	0.886	0.945	0.956	0.892	0.973	0.897	0.897	0.857	0.881	0.898	0.967	0.931	0.930	0.968	0.939
S-8	0.899	0.882	0.940	0.927	0.896	0.911	0.939	0.973	0.963	0.920	0.915	0.915	0.907	0.938	0.874

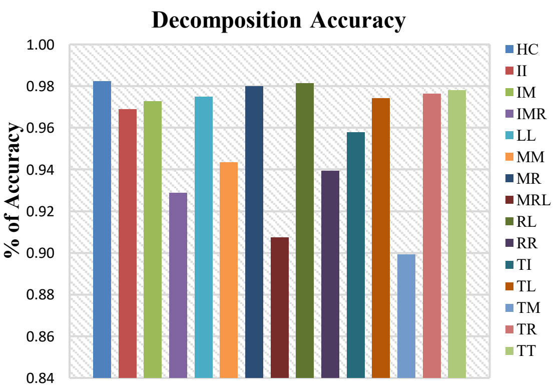

Figure 11. Average decomposition accuracy of different classes of movement (Ch-2)

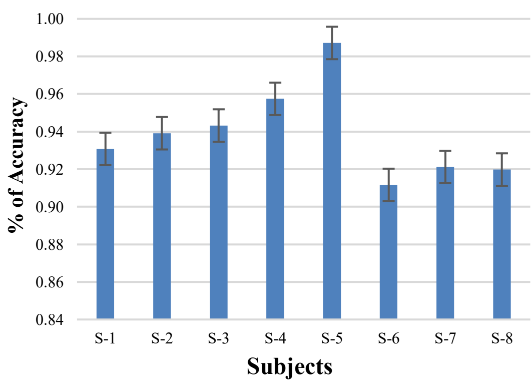

Figure 12. Average decomposition accuracy of different subjects

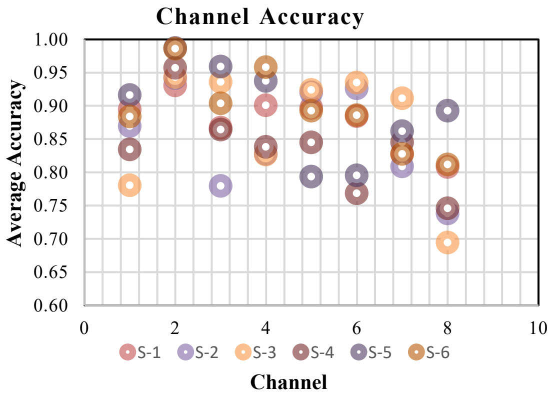

Figure 14. Average decomposition accuracy of different channels

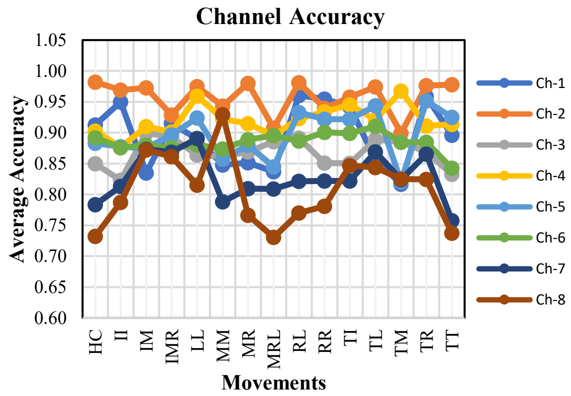

Figure 15. Average decomposition accuracy of different channels for different movement

4. CONCLUSION

Decomposition of EMG signals is challenging due to the complexity and unpredictable nature of muscle activity patterns. Therefore, a comprehensive assessment of signal processing techniques and validation methodologies is required to ensure the correctness and dependability of the results. This paper presents a successful method for multiresolution decomposition and denoising of surface EMG data from fifteen finger movements using the MODWT and a 4th-order Daubechies filter. The most significant finding of this work is the identification of particular frequency bands with the highest levels of motor neuron activation. This finding shows that the quality and interpretability of sEMG signals linked to finger motions are successfully improved by the suggested MODWT-based multiresolution decomposition technique. We also found that the average relative energy of each level remains independent of the movement of any individual or subject. Additionally, the channel selection technique based on average relative energy reduces computational complexity without sacrificing performance, which is essential for embedded and wearable systems that require real-time applications. A correlation examination between the original and reconstructed signals revealed that the average reconstruction and decomposition accuracy was 95.8%. The detection of particular frequency bands that correlate with the firing of motor neurons during finger motions is a remarkable result. This knowledge has physiological ramifications since it can help with the creation of neuromuscular models and neuroprosthetic adaptive control algorithms. As interest in biomedical signal processing and human-centered computing grows, we hope that this research will contribute to improving the functionality of control systems in gesture-based interfaces, rehabilitation equipment, and prosthetics.

FUNDING INFORMATION

This research work was supported by the Startup Fund 2024 by Independent University, Bangladesh (IUB), achieved for the Research Project Number: SU-SETS:24-007.

REFERENCES

[1] B. Mambrito and C. J. De Luca, "A technique for the detection, decomposition and analysis of the EMG signal," *Electroencephalography and Clinical Neurophysiology*, vol. 58, no. 2, pp. 175–188, Aug. 1984, doi: 10.1016/0013-4694(84)90031-2.

[2] S. A. sein Mousavi, M. A. Hasan, M. H. Abdulrazzaq, and M. Naghavizadeh, "Diagnosis of myopathy, neuropathy using electromyogram signal and Wavelet coefficients," in *2020 4th International Symposium on Multidisciplinary Studies and Innovative Technologies (ISMSIT)*, Oct. 2020, pp. 1–3, doi: 10.1109/ismsit50672.2020.9254551.

[3] X. Ren, C. Zhang, X. Li, G. Yang, T. Potter, and Y. Zhang, "Intramuscular EMG decomposition basing on motor unit action potentials detection and superposition resolution," *Frontiers in Neurology*, vol. 9, no. JAN, 2018, doi: 10.3389/fneur.2018.00002.

[4] D. Zennaro, P. Wellig, V. M. Koch, G. S. Moschytz, and T. Laubli, "A software package for the decomposition of long-term multichannel EMG signals using wavelet coefficients," *IEEE Transactions on Biomedical Engineering*, vol. 50, no. 1, pp. 58–69, Jan. 2003, doi: 10.1109/tbme.2002.807321.

[5] J. M. Hahne, M. A. Schweisfurth, M. Koppe, and D. Farina, "Simultaneous control of multiple functions of bionic hand prostheses: Performance and robustness in end users," *Science Robotics*, vol. 3, no. 19, Jun. 2018, doi: 10.1126/scirobotics.aat3630.

[6] C. J. De Luca, A. Adam, R. Wotiz, L. D. Gilmore, and S. H. Nawab, "Decomposition of surface EMG signals," *Journal of Neurophysiology*, vol. 96, no. 3, pp. 1646–1657, Sep. 2006, doi: 10.1152/jn.00009.2006.

[7] F. Negro, S. Muceli, A. M. Castronovo, A. Holobar, and D. Farina, "Multi-channel intramuscular and surface EMG decomposition by convolutive blind source separation," *Journal of Neural Engineering*, vol. 13, no. 2, p. 26027, Feb. 2016, doi: 10.1088/1741-2560/13/2/026027.

[8] M. R. Mohebian, H. R. Marateb, S. Karimimehr, M. A. Mañanas, J. Kranjec, and A. Holobar, "Non-invasive decoding of the motoneurons: a guided source separation method based on convolution kernel compensation with clustered initial points," *Frontiers in Computational Neuroscience*, vol. 13, Apr. 2019, doi: 10.3389/fncom.2019.00014.
[9] A. Del Vecchio, A. Holobar, D. Falla, F. Felici, R. M. Enoka, and D. Farina, "Tutorial: analysis of motor unit discharge characteristics from high-density surface EMG signals," *Journal of Electromyography and Kinesiology*, vol. 53, p. 102426, Aug. 2020, doi: 10.1016/j.jelekin.2020.102426.
[10] H. Zhao, X. Zhang, M. Chen, and P. Zhou, "Online decomposition of surface electromyogram into individual motor unit activities using progressive FastICA peel-off," *IEEE Transactions on Biomedical Engineering*, vol. 71, no. 1, pp. 160–170, Jan. 2024, doi: 10.1109/tbme.2023.3294016.
[11] C. Wei *et al.*, "Recognition of lower limb movements using empirical mode decomposition and k-nearest neighbor entropy estimator with surface electromyogram signals," *Biomedical Signal Processing and Control*, vol. 71, p. 103198, Jan. 2022, doi: 10.1016/j.bspc.2021.103198.
[12] J.-R. Yeh, J.-S. Shieh, and N. E. Huang, "Complementary ensemble empirical mode decomposition: a novel noise enhanced data analysis method," *Advances in Adaptive Data Analysis*, vol. 2, no. 2, pp. 135–156, Apr. 2010, doi: 10.1142/s1793536910000422.
[13] X. Zhang and P. Zhou, "Filtering of surface EMG using ensemble empirical mode decomposition," *Medical Engineering & Physics*, vol. 35, no. 4, pp. 537–542, Apr. 2013, doi: 10.1016/j.medengphy.2012.10.009.
[14] B. Fatimah, P. Singh, A. Singhal, and R. B. Pachori, "Hand movement recognition from sEMG signals using Fourier decomposition method," *Biocybernetics and Biomedical Engineering*, vol. 41, no. 2, pp. 690–703, Apr. 2021, doi: 10.1016/j.bbe.2021.03.004.
[15] C. Chen, S. Ma, Y. Yu, X. Sheng, and X. Zhu, "Segment-wise decomposition of surface electromyography to identify discharges across motor neuron populations," *IEEE Transactions on Neural Systems and Rehabilitation Engineering*, vol. 30, pp. 2012–2021, 2022, doi: 10.1109/tnsre.2022.3192272.
[16] C. Chen, Y. Yu, X. Sheng, D. Farina, and X. Zhu, "Simultaneous and proportional control of wrist and hand movements by decoding motor unit discharges in real time," *Journal of Neural Engineering*, vol. 18, no. 5, p. 56010, Apr. 2021, doi: 10.1088/1741-2552/abf186.
[17] C. Chen, Y. Yu, X. Sheng, and X. Zhu, "Non-invasive analysis of motor unit activation during simultaneous and continuous wrist movements," *IEEE Journal of Biomedical and Health Informatics*, vol. 26, no. 5, pp. 2106–2115, May 2022, doi: 10.1109/jbhi.2021.3135575.
[18] X. Liu, X. Xi, X. Hua, H. Wang, and W. Zhang, "Feature extraction of surface electromyography using wavelet weighted permutation entropy for hand movement recognition," *Journal of Healthcare Engineering*, vol. 2020, pp. 1–11, Nov. 2020, doi: 10.1155/2020/8824194.
[19] F. Duan, L. Dai, W. Chang, Z. Chen, C. Zhu, and W. Li, "sEMG-based identification of hand motion commands using wavelet neural network combined with discrete wavelet transform," *IEEE Transactions on Industrial Electronics*, vol. 63, no. 3, pp. 1923–1934, Mar. 2016, doi: 10.1109/tie.2015.2497212.
[20] A. Phinyomark, C. Limsakul, and P. Phukpattaranont, "Application of wavelet analysis in EMG feature extraction for pattern classification," *Measurement Science Review*, vol. 11, no. 2, Jan. 2011, doi: 10.2478/v10048-011-0009-y.
[21] N. Phukan, N. M. Kakoty, P. Shivam, and J. Q. Gan, "Finger movements recognition using minimally redundant features of wavelet denoised EMG," *Health and Technology*, vol. 9, no. 4, pp. 579–593, May 2019, doi: 10.1007/s12553-019-00338-z.
[22] F. Abramovich, "Wavelet decomposition approaches to statistical inverse problems," *Biometrika*, vol. 85, no. 1, pp. 115–129, Mar. 1998, doi: 10.1093/biomet/85.1.115.
[23] A. Phinyomark, C. Limsakul, and P. Phukpattaranont, "An optimal wavelet function based on wavelet denoising for multifunction myoelectric control," in *2009 6th International Conference on Electrical Engineering/Electronics, Computer, Telecommunications and Information Technology*, May 2009, pp. 1098–1101, doi: 10.1109/ecticon.2009.5137236.
[24] B. Gerdle, S. Karlsson, S. Day, and M. Djupsjöbacka, "Acquisition, processing and analysis of the surface electromyogram," in *Modern Techniques in Neuroscience Research*, Springer Berlin Heidelberg, 1999, pp. 705–755, doi: 10.1007/978-3-642-58552-4_26.
[25] R. N. Khushaba and S. Kodagoda, "Electromyogram (EMG) feature reduction using mutual components analysis for multifunction prosthetic fingers control," in *2012 12th International Conference on Control Automation Robotics & Vision (ICARCV)*, Dec. 2012, pp. 1534–1539, doi: 10.1109/icarcv.2012.6485374.
[26] A. Rahimi, S. Benatti, P. Kanerva, L. Benini, and J. M. Rabaey, "Hyperdimensional biosignal processing: A case study for EMG-based hand gesture recognition," in *2016 IEEE International Conference on Rebooting Computing (ICRC)*, Oct. 2016, pp. 1–8, doi: 10.1109/icrc.2016.7738683.
[27] A. Gijsberts, M. Atzori, C. Castellini, H. Muller, and B. Caputo, "Movement error rate for evaluation of machine learning methods for sEMG-based hand movement classification," *IEEE Transactions on Neural Systems and Rehabilitation Engineering*, vol. 22, no. 4, pp. 735–744, Jul. 2014, doi: 10.1109/tnsre.2014.2303394.
[28] R. N. Khushaba, S. Kodagoda, D. Liu, and G. Dissanayake, "Electromyogram (EMG) based fingers movement recognition using neighborhood preserving analysis with QR-decomposition," in *2011 Seventh International Conference on Intelligent Sensors, Sensor Networks and Information Processing*, Dec. 2011, pp. 1–105, doi: 10.1109/issnip.2011.6146521.
[29] W. Li, P. Shi, and H. Yu, "Gesture recognition using surface electromyography and deep learning for prostheses hand: state-of-the-art, challenges, and future," *Frontiers in Neuroscience*, vol. 15, Apr. 2021, doi: 10.3389/fnins.2021.621885.
[30] T. Guo, T. Zhang, E. Lim, M. Lopez-Benitez, F. Ma, and L. Yu, "A review of wavelet analysis and its applications: challenges and opportunities," *IEEE Access*, vol. 10, pp. 58869–58903, 2022, doi: 10.1109/access.2022.3179517.
[31] S. Al Wadi, A. Hamarsheh, and H. Alwadi, "Maximum overlapping discrete wavelet transform in forecasting banking sector," *Applied Mathematical Sciences*, vol. 7, pp. 3995–4002, 2013, doi: 10.12988/ams.2013.36305.
[32] S. Varshney, D. R. Thakur, and R. Jigyasu, "EMG signal based pattern recognition of grasping movement using MODWT and weighted k-nearest neighbor," *International Journal of Innovative Technology and Exploring Engineering*, vol. 8, no. 10, pp. 1759–1764, Aug. 2019, doi: 10.35940/ijitee.j9137.0881019.
[33] A. A. A. Dghais and M. T. Ismail, "A comparative study between discrete wavelet transform and maximal overlap discrete wavelet transform for testing stationarit," *International Journal of Mathematical Science and Engineering*, vol. 7, no. 12, pp. 1677–1681, 2013.
[34] D. B. Percival and A. T. Walden, *Wavelet Methods for Time Series Analysis*. Cambridge University Press, 2000, doi: 10.1017/CBO9780511841040.
[35] M. J. A. Bolzan, F. L. Guarnieri, and P. C. Vieira, "Comparisons between two wavelet functions in extracting coherent structures from solar wind time series," *Brazilian Journal of Physics*, vol. 39, no. 1, Mar. 2009, doi: 10.1590/s0103-97332009000100002.
[36] C. Stolojescu, I. Railean, S. Moga, and A. Isar, "Comparison of wavelet families with application to WiMAX traffic forecasting," in *2010 12th International Conference on Optimization of Electrical and Electronic Equipment*, May 2010, pp. 932–937, doi: 10.1109/optim.2010.5510403.

[37] S. Upadhyaya, "Implementation of maximal overlap discrete wavelet transform and S-transform for localization of power quality disturbance signals," *International Journal of Applied Engineering Research*, vol. 14, no. 13, pp. 2989–2994, 2019.
[38] T. Q. Nguyen, "Separation of the structure signal by the maximal overlap discrete wavelet transform and fast Fourier transform," *Advances in Materials Science and Engineering*, vol. 2021, no. 1, Jan. 2021, doi: 10.1155/2021/3328684.
[39] A. Sultana, M. T. I. Opu, F. Ahmed, and M. S. Alam, "A novel machine learning algorithm for finger movement classification from surface electromyogram signals using welch power estimation," *Healthcare Analytics*, vol. 5, p. 100296, Jun. 2024, doi: 10.1016/j.health.2023.100296.

BIOGRAPHIES OF THE AUTHORS

Afroza Sultana received her B.Sc. and M.Sc. in 1997 and 1998 from the Department of Applied Physics and Electronics (now named electrical and electronic engineering) of the University of Dhaka. She received her second M.Sc. in telecommunication engineering from Independent University, Bangladesh (IUB) in 2008. She is working on her Ph.D. in biomedical signal processing from the Department of Electrical and Electronic Engineering (EEE), University of Dhaka. After graduating from the University of Dhaka, she started her career as a lecturer of computer science at the Microland International Institute of Computer Education (IICE) in 1999. She began working with Independent University, Bangladesh (IUB) in April 2000 and is currently serving as a senior lecturer in the Department of EEE. Her research interests include biomedical signal processing, machine learning, sensor networks and computer networking, and digital electronics. She has published a good number of research works in reputed international journals and conferences. She can be contacted at email: afroza@iub.edu.bd.

Md. Tawhid Islam Opu completed his B.Sc. electrical and electronic engineering from Independent University, Bangladesh (IUB) in the year 2019 and is currently pursuing his M.Sc. degree in electrical and electronic engineering from Independent University, Bangladesh (IUB), Dhaka, Bangladesh. His research interests include artificial intelligence, machine learning, biomedical instrumentation and signal processing, agricultural advancement, smart systems, automation, and robotics. He can be contacted at email: md.tio971125@gmail.com.

Md. Shafiul Alam is working as a professor in the Department of Electrical and Electronic Engineering, the University of Dhaka. He obtained his Ph.D. from the Department of Automatic Control and Systems Engineering, University of Sheffield, UK, in 2007 under the Commonwealth Fellowship scheme. He completed B.Sc. (Hons) and M.Sc. degrees in applied physics and electronics from the University of Dhaka, Bangladesh. His research interests include robotics and control engineering, intelligent control of robotic arms and unmanned vehicles, artificial intelligence, fuzzy logic, neural networks, deep learning, evolutionary algorithms, biomedical engineering, systems biology, and embedded systems. Dr. Alam worked as a post-doctoral researcher at the University of Northumbria at Newcastle, UK, and at Anglia Ruskin University, UK, under the Commonwealth Fellowship Program. He also worked as a post-doctoral researcher at Bradford University, UK. Dr. Alam worked as a visiting professor in the School of Electrical and Electronic Engineering at the University of Science (USM), Malaysia. He can be contacted at email: msalam@du.ac.bd.

Farruk Ahmed is a professor at the Department of Computer Science and Engineering of Independent University, Bangladesh. He is a former renowned professor of applied physics and electronics (now the Department of EEE) at the University of Dhaka and North South University (NSU). He obtained his Ph.D. from the University of Salford, Manchester, England, in 1979. He started his career as a lecturer at the University of Dhaka in 1967. He is the former president of the Bangladesh Electronic Society. He has supervised a good number of Ph.D. students and many graduate and undergraduate theses. He has published a lot of research articles in many national and international journals and conferences. He can be contacted at email: farruk@iub.edu.bd.